Residual strain evaluation of curved surface by grating-transferring technique and GPA

Zhanwei Liu,[1, a)] Jiangfan Zhou,[1] Xianfu Huang,[1] Jian Lu,[2] and Huimin Xie[3, b)]
[1)] *Department of Mechanics, School of Astronautics, Beijing Institute of Technology, Beijing 100081, China*
[2)] *Department of Mechanical Engineering, The Hong Kong Polytechnic University, Hong Kong, China*
[3)] *AML, Department of Engineering Mechanics, Tsinghua University, Beijing 100084, China*

(Received 19 July 2011; accepted 02 August 2011; published online 10 September 2011)

Abstract This paper investigates an advanced grating-transferring technique combined with geometric phase analysis (GPA) for residual strain evaluation of curved surface. A standard holographic grating is first transferred to a pre-produced epoxy resin film and then consolidated to a test region of curved surface. With a rubber mold and silicone rubber the deformed grating is replicated to a sheet metal after hole-drilling for release of residual stress. After that the grating is transferred from the sheet metal to the glass plate, which would be served as an analyzer grating (specimen grating). By GPA the local strain distributions related to the phase difference between the reference grating and analyzer grating for the released stress can be evaluated. A validation test has been conducted on the weld joint of a stainless steel tube and the obtained results demonstrate the ability of the method in measuring the residual strain of curved surface. [doi:10.1063/2.1105107]

Keywords residual strain, grating-transferring, hole-drilling, GPA, curved surface

In the last decades, lots of advanced and proven techniques with high quality and good performance have been developed to evaluate one of the most important characters in machining field—residual stress, such as hole-drilling method, sectioning method, indentation-strain method, X-ray and neutron diffraction methods and so on.[1–5] Of all these methods the most widely used hole-drilling method usually couples with conventional strain rosettes to measure strain values in some fixed-points (typically there are three directions: two orthogonal and one shear directions). The method is of high precision, but it is not suitable for the full-field measurement and in complex curved surface. An alternative approach to settle this problem is using optical methods to reveal deformation of full-field which is well suitable for curved surface. Li[6] has employed optical strain rosettes instead of resistance strain gages to reveal full-field local strain distributions, which is much convenient and visually perceivable. Buitrago et al.[7] have developed a transferring technique to measure in-plane strain on curved surface. Zou et al.[8] have investigated the residual strain of laser welding specimen by high temperature resistant gratings. McDonach et al.[9] have proposed an improved moire interferometry with combination of hole-drilling method to measure residual stress. In general the aforementioned works are really remarkable in two or three aspects, but there are still some shortcomings such as they are experimentally and operationally difficult and also result in low efficiency.

This paper intends to provide an advanced grating-transferring technique combined with hole-drilling method and GPA[10–12] to measure residual strain of curved surface. With GPA the difference between reference grating and specimen grating could be evaluated after stress released by hole-drilling. This improved technique is outstanding for easily operating and full-field, as well as high precision and accuracy.

To achieve the deformation fields on the curved surface, a grating-transferring technique is developed based upon conventional transferring techniques,[13] whose technological process is illustrated in Fig. 1. Briefly, a standard holographic grating (reference grating) was first transferred to a prepared epoxy resin film and then adhered to the test surface. After drilling the curved grating was replicated to a sheet metal and then transferred to a glass plate as analyzer grating (specimen grating). By analyzing the difference between the reference grating and specimen grating the deformation fields could be evaluated.

In the following reports each subdivision will be discussed in detail.

Mix the epoxy resin (XY508), curing agent and the flexibilizer (DBP) homogeneously with the proportion of 20 : 5 : 2. As the mixture is first air bubbles removed in the centrifugal separator and then firmly compacted with a uniform pressure according to the following arrangement (as shown in Fig. 2), epoxy resin film is acquired after the solidification of epoxy glue.

Similar to the process of the epoxy resin film, the same mixture (epoxy resin, curing agent and flexibilizer) is first air bubbles removed and then poured onto the cleared epoxy resin film. With firmly compacted the standard holographic grating to the processed epoxy resin film, an epoxy resin grating film could be obtained after the solidification of epoxy glue, as vividly illustrated in Fig. 3.

The obtained grating film is then adhered to the test location by 502-glue, which would be served as a

[a)]Email: liuzw@bit.edu.cn.
[b)]Corresponding author. Email: xiehm@mail.tsinghua.edu.cn.

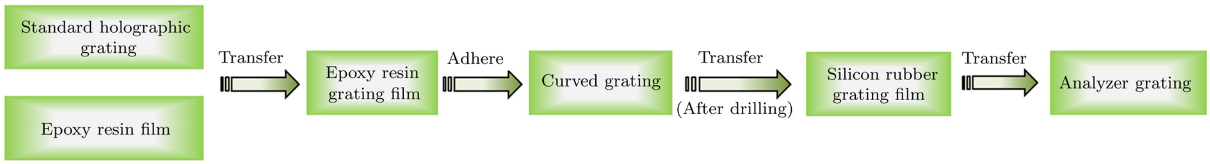

Fig. 1. Flow path of the transferring technique.

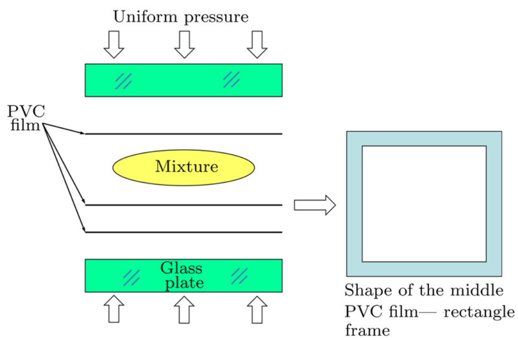

Fig. 2. Forming process of the epoxy resin film.

deformation carrier during the stress releasing courses.

The silicon rubber is selected as the transferring medium of curved grating for its outstanding behaviors of easiness and simplicity to handle and less impact on the deformed grating. Detailed procedures are listed as follows:

(1) The sheet metal (beryllium bronze slice, 0.1 mm) is first oxide layer polished and then coupling agent processed.

(2) Mix room temperature vulcanized silicone rubbers (RTV, 106# or 107#) with curing agent (TEOS) homogeneously according to the proportion of 20:1. With the air bubbles removed in the centrifugal separator, the slice with silicon rubber coated is firmly compacted to the curved surface by a rubber mold (as shown in Fig. 4). The silicon rubber is suggested as thin as possible to cooperate with the slice to cut down the air bubbles. Take off the deformed grating film after the solidification of silicon rubber.

(3) The beryllium bronze slice and the silicon rubber are easily resiled due to their advanced rebound resilience under room temperature. Since the silicon rubber grating is hardly to preserve, usually a stable analyzer grating by transferring the grating to the epoxy glue is necessary, as illustrated in Fig. 5.

There would be virtual strain during the grating-transferring process which will influence the true strain values of the measurement. To eliminate its harmful effect an experiment was conducted on the undrilled specimen to estimate the virtual strain. Firstly, a standard holographic grating (reference grating) was transferred to a prepared epoxy resin film which would then be adhered to the curved surface to be served as deformation carrier. Then the curved grating film was replicated to a sheet metal and finally transferred to a glass plate to be served as analyzer grating (specimen grating). The differences between the reference grating (1 200 line/mm) and the analyzer grating (transferred from the undrilled specimen) were evaluated by GPA, which were exactly the virtual strain, as shown in Fig. 6 and Table 1.

Table 1. Virtual strain

Virtual strain	ε_X	ε_Y	γ_{XY}
Mean value	–0.001 5	0.001 8	–0.000 4

From the obtained results it can be concluded that the average virtual strain values were overall less than 0.002 (0.2%), which indicated some defects (air bubbles or some others) during grating transferring process. It should be removed in calculation to get the actual strain values, which will be discussed in detail in the next subsection.

The strain values of curved grating in cylindrical coordinate system (denoted as ε_c) are different from that of analyzer grating in plane coordinate system. As referred to the replication schematic diagram illustrated in Fig. 6, their relation could be written as[13]

$$\varepsilon_c = \frac{(1+\varepsilon'')\left(1+\dfrac{\delta'+\delta_2/2}{R_1'}\right)}{(1+\varepsilon')\left(1+\dfrac{\delta''+\delta_2/2}{R_1''}\right)} - 1, \tag{1}$$

where ε' is the virtual strain value of analyzer grating transferred before drilling and ε'' is the strain value of analyzer grating transferred after drilling, respectively; both ε' and ε'' are measured in plane coordinate system; δ' and δ'' are the thickness of silicon rubber before and after drilling respectively; δ_2 is the thickness of sheet metal; R_1' and R_1'' are the radius of curvature of the curved specimen before and after hole drilling respectively, as shown in Fig. 7. (Note: superscripts " $'$ " and " $''$ " are variables before and after hole drilling, respectively.)

This brief formula indicates the basic relationship of the strain values in plane coordinate system and cylindrical coordinate system.

Residual stress in welded joints[14] is a key issue which determines the fracture behaviors of the devices or structures. In this paper a stainless steel tube welded by an argon-arc welding joint was selected as the test specimen, as shown in Fig. 8(a). The welding speed was 31.4 mm/min and the filler was 304 welding flux. To minimize the vibration during drilling, the experi-

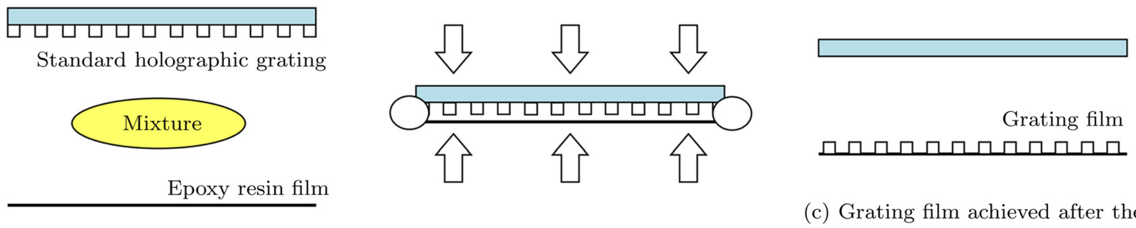

(a) Working scheme

(b) Firmly compacted the processed film to the standard holographic grating

(c) Grating film achieved after the solidification of epoxy glue and opening mould process of (b)

Fig. 3. Process of the epoxy resin grating film.

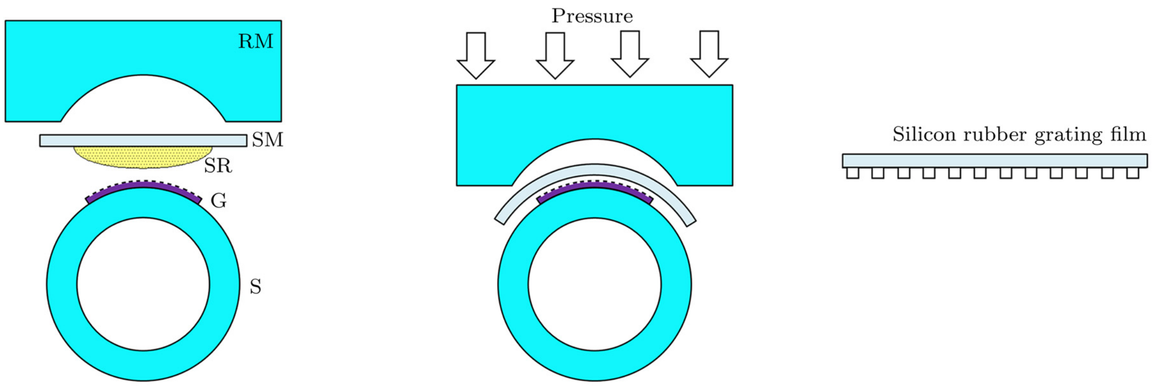

(a) Working scheme, RM: Rubber mold, SM: sheet metal, SR: silicon rubber, G: curved grating film, S: steel tube

(b) Firmly compacted

(c) Silicon rubber grating film after the solidification of silicon rubber and opening mould process of (b)

Fig. 4. Replication of the curved grating.

ment system was set up on a vibration isolator. Since the drilling machine (with a drill diameter of 1 mm, i.e. $r_0 = 1$ mm) was fixed, a translation stages with a spatial resolution of 1 μm was employed as the feed system. The experiment setup was shown in Fig. 8(b) and the general layout of the experimental setup was shown in Fig. 8(c).

(1) Adhere the prepared grating film to the test location, and then drilling.

(2) Transfer the deformed grating to the silicon rubber after drilling (stress released).

(3) Replicate the silicon rubber grating to the epoxy resin to fabricate the analyzer grating.

(4) Observe the coated analyzer grating under the optical microscope, and then capture the images. Analyze the collected images by GPA, strain distributions along specific drilling depth would be revealed.

(5) Repeat the above courses five times with the drilling depth of 0 mm, 0.4 mm, 0.6 mm, 0.8 mm and 1.0 mm, respectively.

The collected images were processed by GPA and the strain distributions (ε_X and ε_Y) along different drilling depths were shown in Fig. 9. In this discussion a region located at $1.20r_0$ away from the drilling-hole center with the area of 70 μm × 50 μm was selected to investigate.

Then the average strain distributions (ε_X, ε_Y, and γ_{XY}) along the drilling depths were evaluated after numerical fitting, as illustrated in Fig. 10.

In summary the distribution of ε_X first decreased in the range of 0.40∼0.75 mm and then increased in the range of 0.75∼0.90 mm. While as to the distribution of ε_Y, it first increased in the range of 0.40∼0.50 mm and then decreased in the range of 0.50∼0.80 mm. With the increase of the depth, the strain would decrease and finally it was close to zero. The maximum value is negative ($\approx -0.012\,5$, compressive strain) located at the depth of 0.50 mm. While the non-striking changes of shear strain along the depths indicated the less impact of the welding on the shear stress.

High quality grating films based upon transferring technique have been discussed in detail and established to measure the residual strain fields of curved surface with combination of advanced GPA in this investigation. A validation test has been conducted. Repeatable and reliable experiments demonstrate the superior performance of the technique. It is easily accessible, environmental adaptable and almost no apparatuses are specially required, which enables the widely applications for industrial use.

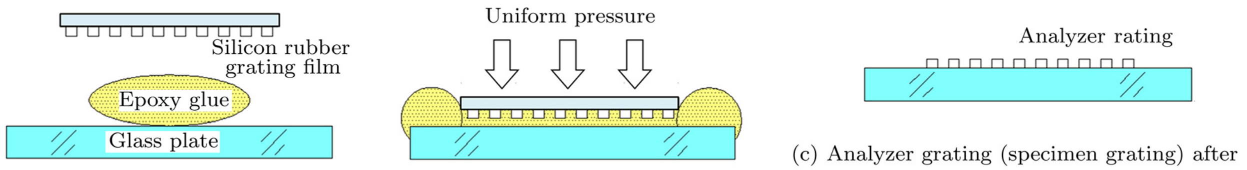

(a) Working scheme (b) Firmly compacted (c) Analyzer grating (specimen grating) after the solidification of epoxy glue and opening mould of process of (b)

Fig. 5. Transferring of the analyzer grating.

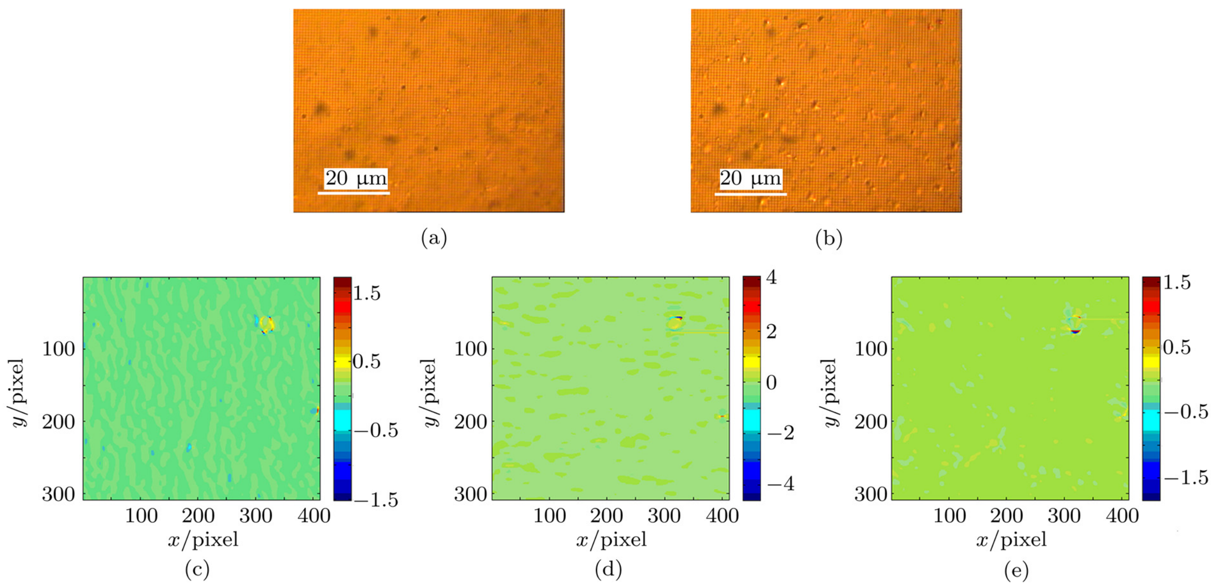

Fig. 6. Virtual strain distributions evaluated by GPA after grating transferred from the undrilled curved specimen, (a) reference grating; (b) analyzer grating transferred from the silicon rubber grating film; (c), (d) and (e) local strain distributions ε_X, ε_Y and γ_{XY}, respectively.

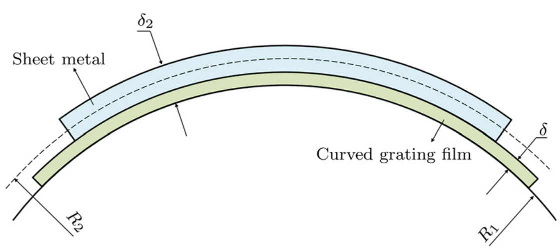

Fig. 7. Replication of the curved grating.

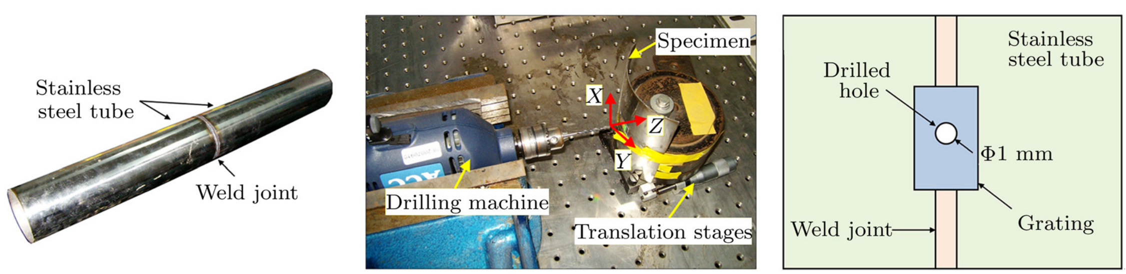

(a) (b) (c)

Fig. 8. (a) Specimen to be measured: stainless steel tube (length × OD × thickness = 80 cm × 10 cm × 1 mm) welded by an argon-arc welding joint (length = 5 mm); (b) experiment system and (c) general layout (plan view) of the experimental setup on the specimen.

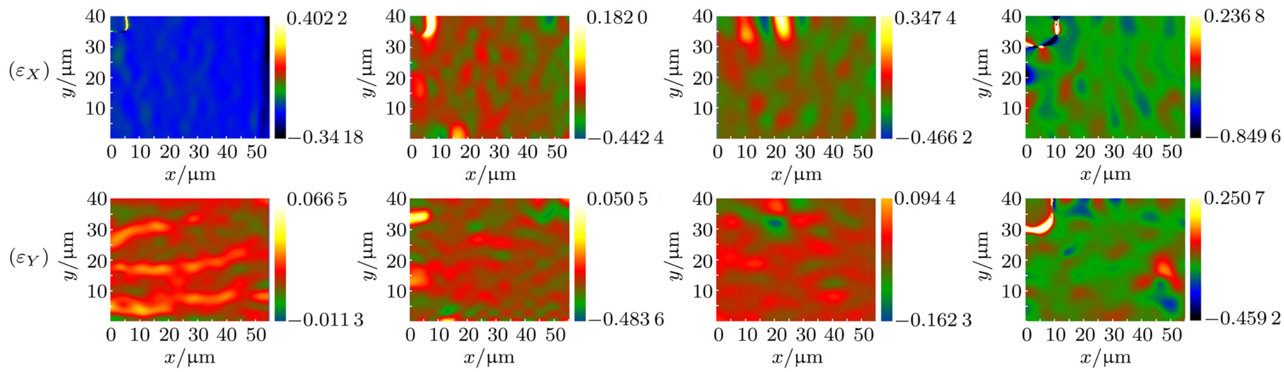

(a) $h = 0.2$ mm (b) $h = 0.4$ mm (c) $h = 0.8$ mm (d) $h = 1.0$ mm

Fig. 9. Residual strain distributions (ε_X and ε_Y) along different drilling depths.

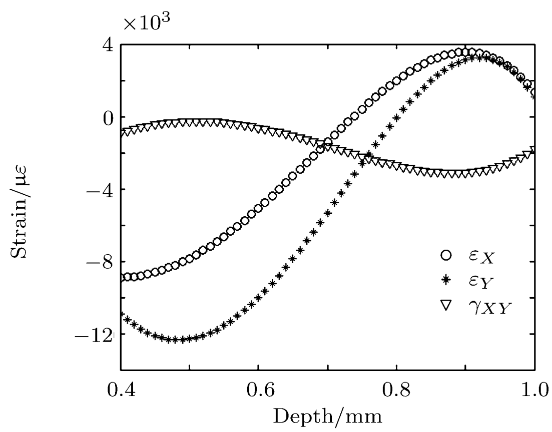

Fig. 10. Strain distributions along the drilling depth.

This work was supported by the National Natural Science Foundation of China (11072033 and 90916010) and Specialized Research Fund for the Doctoral Program of Higher Education (20090002110048).

1. M. T. Flaman, and B. H. Manning, Exp. Mech **25**, 205 (1985).
2. E F Rybicki, and J R Shadley, J. Eng. Mater. Technol. **108** 99 (1986).
3. J. G. Swadener, B. Taljat, and G. M. Pharr, J. Mater. Res. **16**, 2091 (2001).
4. J. Lu, and D. Retraint, J. Strain Anal. Eng. **33**, 127 (1998).
5. A. J. Allen, M. A. Bourke, and S. Dawes, et al, J. Acta Metall. Mater. **40**, 40 (1992).
6. K. Y. Li, Solid Mech. Appl. **82**, 145 (2002).
7. J. Buitrago, A. J. Durelli, and V. J. Park, J. Strain Anal. Eng. **13**, 121 (1978).
8. D. Q. Zou, H. M. Xie, and G. T. Wang, et al, J. Tsinghua Univ. (Sci & Tech) **37**, 58 (1997) (in Chinese).
9. A. McDonach, J. Mckelvie, and P. Mackenzie, et al, Exp. Tech. **7**, 20 (1983).
10. M. J. Hÿch, and L. Potez, Phil. Mag. A **76**, 1119 (1997).
11. Z. W. Liu, H. M. Xie, and C. Z. Gu, et al, J. Micromech. Microeng. **19**, 015012 (2009).
12. Z. W. Liu, H. M. Xie, and D. N. Fang, et al, Appl. Phys. Lett. **87**, 201908 (2005).
13. D. Q. Zou, [Ph.D. Dissertation], (Tsinghua University, Beijing, 1996) (in Chinese).
14. D. J. Kong, Y. Z. Wu, and D. Long, et al., Theor. Appl. Mech. Lett. **1**, 031008 (2011).